

# Fourier synthesis of optical potentials for atomic quantum gases

Gunnar Ritt\*,<sup>1,2</sup> Carsten Geckeler,<sup>1</sup> Tobias  
Salger,<sup>1,2</sup> Giovanni Cennini,<sup>1</sup> and Martin Weitz<sup>1,2</sup>

<sup>1</sup>*Physikalisches Institut der Universität Tübingen,  
Auf der Morgenstelle 14, 72076 Tübingen, Germany*

<sup>2</sup>*Institut für Angewandte Physik der Universität Bonn,  
Wegelerstraße 8, 53115 Bonn, Germany*

(Dated: February 19, 2019)

PACS numbers: 03.75.Lm, 32.80.Lg, 32.80.Wr, 42.50.Vk

Optical lattices have developed into successful model systems for solid state physics problems. In such systems, effects like Bloch-oscillations and the Mott-insulator transition were observed [1, 2]. On the other hand, current quantum gas experiments with optical lattices have been limited to sinusoidal atom potentials. Recent theoretical work pointed out that in unconventional lattice structures novel quantum phases are expected [3, 4]. We here demonstrate a scheme to create dissipationless optical lattice potentials with  $\lambda/2n$  spatial periodicity, where  $n$  is an integer number. In a proof-of-principle experiment carried out with a rubidium Bose-Einstein condensate, a lattice potential with  $\lambda/4$  spatial periodicity is realized with a fourth-order Raman process. By combining the  $\lambda/4$  period multiphoton potential with a conventional lattice potential of  $\lambda/2$  spatial periodicity with appropriate phase, an asymmetric lattice with variable asymmetry is Fourier synthesized. The scheme is scalable, in principle, to arbitrarily many Fourier components.

The properties of solid state materials are much determined by the internal spatial structure of its constituents. Most natural solid state materials are crystals, in which the constituents are spatially ordered following the principle of lattice structures. A large class of different unit cells is known, whose classification into crystal classes, point- and space groups is well established within the field of crystallography [5]. Recently, artificial crystals of atoms bound by light, so called optical lattices, have developed into model systems for solid state physics problems. These optical lattices have been limited to sinusoidal atom potentials, with the lattice periodicity determined by half the wavelength of the used trapping light.

A possible way to at least in one dimension produce arbitrarily shaped potentials is the use of beams that are inclined under different angles, which may seem impractical and hard to phase stabilize especially if larger numbers of beams are required. Notably, such phase stabilization has recently been achieved for two near-resonant standing waves [6]. For thermal atoms some nonstandard optical lattices, as subwavelength structure potentials or asymmetric lattices, have been realized with magneto-optical potentials or grey lattices [7, 8]. These schemes require near-resonant optical radiation whose inherent dissipation impedes the use of quantum degenerate atomic gases. With the so far demonstrated schemes, the class of realizable lattice potentials furthermore seems limited.

Here, we demonstrate a scheme to create dissipationless optical lattice potentials with

$\lambda/4$  spatial periodicity, which is realized with a fourth-order Raman process. Building upon this potential, a Fourier synthesis of lattice potentials is demonstrated. By combining the  $\lambda/4$  period multiphoton potential with a conventional lattice of  $\lambda/2$  spatial periodicity with appropriate phase, an asymmetric lattice with variable asymmetry is realized. The scheme for the generation of the  $\lambda/4$  period lattice potential is generalizable, in principle, to optical lattice potentials with  $\lambda/2n$  spatial periodicity, where  $n$  is an integer number. By diffraction of a rubidium Bose-Einstein condensate at the optical light shift potential, absorption images of atom clouds closely connected to the reciprocal lattice of the synthesized potential structures were observed.

In conventional optical lattices with two counterpropagating beams of wavelength  $\lambda$ , the resulting optical potential  $V(z) = -(\alpha/2)|E(z)|^2$ , with  $\alpha$  as the atomic polarizability, is proportional to  $\cos^2 kz = (1 + \cos 2kz)/2$ , yielding the well-known  $\lambda/2$  spatial periodicity. The atoms here undergo virtual two-photon processes of absorption of a photon from one laser beam and stimulated emission into the counterpropagating beam. For a Fourier synthesis of arbitrarily shaped potentials, the required higher harmonics can, in principle, be generated by using a combination of standing waves with wavelengths of the fractional harmonics  $\lambda/n$ , where  $n$  is integer, yielding a lattice potential of spatial period  $\lambda/2n$ . A lattice potential of the same periodicity could also be produced, in case each virtual absorption or stimulated cycle could be replaced by a simultaneous process induced by  $n$  photons of the fundamental wavelength  $\lambda$  absorbed or emitted along the corresponding direction (see Fig. 1 a). The spatial period of this higher order lattice potential can be expressed as  $\lambda_{\text{eff},n}/2 = \lambda/2n$ , where  $\lambda_{\text{eff},n} = \lambda/n$  denotes the effective wavelength of a  $n$ -photon field. A direct measurement of this effective multiphoton wavelength is in general a very difficult task, as has been discussed in the context of Heisenberg-limited measurements [9]. We here use the high frequency resolution of Raman transitions between ground state sublevels to separate in frequency space the desired  $2n$ -th order process from lower order contributions. Theoretical work has predicted, that a lattice potential of  $\lambda/2n$  spatial periodicity is indeed expected with this approach [10, 11, 12]. Fig. 1 b shows the used scheme for a four-photon lattice, which yields a periodic potential with  $\lambda/4$  spatial periodicity. The scheme uses three-level atoms with two stable ground states  $|g_0\rangle$  and  $|g_1\rangle$  and one electronically excited level  $|e\rangle$ . Compared to the four-photon ladder scheme (right graph of Fig. 1 a), one absorption and one stimulated emission process have been interchanged by a stimulated emission and

absorption process of an oppositely directed photon respectively. To avoid second order standing wave processes, a minimum of three laser frequencies is required. The atoms are irradiated with two driving optical fields of frequencies  $\omega \pm \Delta\omega$  from the left and one field with frequency  $\omega$  from the right. A non-zero two-photon detuning  $\delta$  is used to suppress resonant Raman processes. The adiabatic light shift potential for e.g. atoms in state  $|g_0\rangle$  here exhibits the desired fourth-order energy shift  $V \propto (1 + \cos 4kz)$  with spatial periodicity  $\lambda/4$  [10, 11, 12]. In an atom optics picture, the obtained  $\lambda/4$  spatial periodicity can be understood by considering the momentum transfer to an atom during virtual four-photon cycles of alternating absorption and stimulated emission which is  $\pm 4\hbar k$ , being a factor 2 above the corresponding processes in a standing laser wave. By combining lattice potentials of different spatial periodicities, in principle, arbitrarily shaped periodic potentials can be generated. The used scheme for such a Fourier synthesis is visualized in Fig. 2.

In our experimental setup, light detuned some 2 nm to the red of the rubidium D2-line is generated by a diode laser source and subsequently split into two beam paths, from which two counterpropagating beams realizing the variable lattice potential are derived (see methods). The different optical frequencies required to produce a multiphoton lattice can be generated in one beam by driving an acousto-optical modulator with several radio frequencies simultaneously. Both beams are focused in a counterpropagating geometry onto a  $^{87}\text{Rb}$  Bose-Einstein condensate (BEC) confined in a CO<sub>2</sub>-laser dipole trap. After the generation of the BEC, the lattice beams are activated for a period  $T \simeq 6\mu\text{s}$ . To read out the spatially varying potential of the multiphoton lattice, we study the far-field diffraction pattern of the imprinted phase grating after a free falling time of 10 ms. From the measured diffraction patterns, we can reconstruct the optical potential.

By choosing variable amplitudes and phases of the lattice potentials, different lattices were Fourier synthesized. To begin with, we investigated a conventional optical lattice. Fig. 3 a shows a typical obtained absorption image along with the reconstructed potential. For this measurement, only two counterpropagating beams with frequency  $\omega$  were required. Fig. 3 b shows corresponding results obtained for the four-photon lattice potential, as realized with the scheme shown in Fig. 1 b. For this measurement, two beams with frequency  $\omega \pm \Delta\omega$  and one counterpropagating beam with frequency  $\omega$  were activated. The main peaks of the absorption image here are spatially separated by twice the amount shown in Fig. 3 a, which reflects the by a factor two smaller spatial periodicity of  $\lambda/4$  of this four-photon lattice.

To demonstrate a Fourier synthesis of atom potentials, two- and four-photon lattice potentials were overlapped. Here, all four light fields were used (see Fig. 2), so that in addition to the optical frequency components shown in Fig. 1 b also a counterpropagating beam with frequency  $\omega$  was active. By changing the phase of the control beam with frequency  $\omega$  with respect to the other beams, the phase of the four-photon contribution could be varied relatively to the position of the two-photon potential. Fig. 3 c and Fig. 3 d show far-field diffraction patterns and the reconstructed unit cells for such lattices. For the measurement shown in Fig. 3 d, the phase of the four-photon contribution was changed by  $180^\circ$  with respect to that shown in Fig. 3 c. In both images the diffraction pattern is clearly asymmetric, especially when considering the amplitude of the  $\pm 2\hbar k$  peaks. This is attributed as evidence for asymmetric atom potentials, as also visible in the shown reconstructed lattice potentials.

We have also investigated diffraction patterns from lattice potentials with a more complete range of phase shifts of the four-photon potential. As the fundamental period of the combined lattice is  $\lambda/2$ , we anticipate that the relative magnitude of the  $\pm 2\hbar k$  diffraction peaks gives an indication for the asymmetry of the lattice potential. Fig. 4 shows the fraction of atoms diffracted into the  $\pm 2\hbar k$  orders relatively to the total number of atoms as a function of the phase shift. The data points have been fitted with sinusoidal functions which is in accordance with theory for small pulse envelopes (see methods). One clearly observes the variation of asymmetry of the diffraction pattern as a function of the phase between the different Fourier components.

To conclude, we report on the realization of atom potentials suitable for atomic Bose-Einstein condensates with spatial periodicity  $\lambda/4$  using multiphoton Raman transitions. This has allowed us to demonstrate a scheme for the Fourier synthesis of asymmetric shaped, conservative lattice potentials. The scheme is generalizable to generate, in principle, arbitrarily shaped periodic optical potentials. In future, it would be interesting to extend this scheme to include even smaller period lattice potentials. Besides in the search for new quantum phases, tailored high-periodicity lattices are of interest e. g. in the context of subhealing length physics, atom lithography [13] and quantum computing [14]. An intriguing other perspective includes studies of quantum ratchets with atomic quantum gases. It is expected that the investigation of the extremely weakly damped regime, in which the atomic inertia plays a large role, will allow for novel quantum dynamical phenomena [15].

## I. METHODS

### A. Experimental setup and procedure

Our  $^{87}\text{Rb}$  Bose-Einstein condensate (BEC) is produced all-optically by evaporative cooling in a tightly focused  $\text{CO}_2$ -laser beam operating near a wavelength of  $10.6\ \mu\text{m}$ , as described in detail in [16]. By activating a magnetic gradient field during the evaporation phase, a spin-polarized condensate with approximately 10,000 atoms in the  $m_F = -1$  Zeeman state of the  $F = 1$  ground state is produced. The variable lattice potential is generated with the radiation (wavelength 782.4 nm) of a high-power diode laser system. The emitted radiation is split into two beams (beam 1, beam 2), from which, after passing independent acousto-optical modulators (AOM 1, AOM 2), the two counterpropagating beams realizing the lattice potentials are derived. The AOMs are used for switching of the optical fields and in the case of beam 2, to superimpose several optical frequency components onto a single beam path. To generate the rf drive signals for the AOMs, we use a set of four phase-locked function generators. While AOM 1 is driven with a single radio frequency, for AOM 2, the radio frequency signals of three function generators are combined. In this way, the three different optical frequencies required to synthesize the asymmetric lattice can be generated in beam 2. After passing the AOMs, the two beams are fed through optical fibers and focused in a counterpropagating geometry onto the BEC confined in the  $\text{CO}_2$ -laser dipole trap. The typically used optical lattice beam powers are 18 mW for the frequency components  $\omega \pm \Delta\omega$ , and 24 mW (4 mW) for the components with frequency  $\omega$  in beam 1 (beam 2) on a  $40\ \mu\text{m}$  beam waist. The optical lattice beams are inclined under an angle of  $41^\circ$  respectively to the horizontally orientated  $\text{CO}_2$ -laser trapping beam.

A magnetic bias field generates a frequency splitting  $\omega_Z/2\pi \approx 805\ \text{kHz}$  between neighboring Zeeman ground states of the rubidium atoms. For a typical optical frequency difference  $\Delta\omega/2\pi = 930\ \text{kHz}$  we arrive at a Raman detuning  $\delta/2\pi \approx 125\ \text{kHz}$ . The magnetic bias field forms an angle with respect to the optical beam axis, so that the atoms experience both  $\sigma^+$ ,  $\sigma^-$ , as well as  $\pi$  polarizations. To realize the multiphoton lattice as shown in Fig. 1b, we use the  $F = 1$  ground state levels  $m_F = -1$  and  $m_F = 0$  as states  $|g_0\rangle$  and  $|g_1\rangle$  respectively and the  $5\text{P}_{1/2}$  manifold as the electronically excited state  $|e\rangle$ . Since the lattice beam detuning is orders of magnitude larger than the upper state hyperfine structure splitting,

Raman transitions only couple neighboring ground state Zeeman levels. For alkali atoms, the Raman lattice detuning is limited to a value of order of the excited state fine structure splitting ( $\approx 15$  nm for Rb, 34 nm for Cs), which for these atoms for typical parameters limits the expected coherence time of the multiphoton lattice to a value of order of a second due to photon scattering. Longer coherence times should be possible e.g. with the use of metastable P-triplett states of two-electron atoms, as e.g. the  ${}^3P_2$  state in atomic ytterbium with 17 s life time, an atom with which BEC has recently been achieved [17].

### B. Analysis of the diffraction pattern

As is well known from crystal structure analysis, measurements of the intensity of a scattered or diffracted beam, do not in general allow one to reconstruct the lattice structure, as is known as the phase problem. For many special cases, a reconstruction is however possible [18]. In our experiment, assuming that the one-dimensional lattice is invariant to spatial translations of  $\lambda/2$ , the reciprocal lattice is limited to the harmonics  $\lambda/2n$  and it is straightforward to show that a measurement of the atom diffraction pattern  $W(p) = |\Psi(p)|^2$  allows one to reconstruct the spatial lattice structure.

We have fitted the result of a numerical solution of the time-dependent, momentum-picture Schrödinger equation to our experimental far-field diffraction data. The used Hamiltonian was  $H = p^2/2m + V(z)$ , where  $V(z) = \frac{V_1}{2} \cos(2kz) + \frac{V_2}{2} \cos(4kz + \Phi)$ . For known phase  $\Phi$  and pulse length  $T$ , the potential depths  $V_1$  and  $V_2$  of the two- and four-photon lattice components were left as free parameters and could thus be determined from the fit. The reconstructed potentials are shown in Fig. 3 for several different lattices.

Interestingly, we found no major difference between these results and an analytical solution for the atomic diffraction pattern obtained using the simple thin grating (Raman-Nath) approximation (roughly below 20% difference). In the Raman-Nath approximation, the kinetic energy in the Hamiltonian is neglected, which requires (1)  $T \ll 1/\omega_{\text{rec}}$ , where  $\omega_{\text{rec}}$  is the recoil frequency, and (2)  $T \ll T_{\text{osc}}/4$ , where  $T_{\text{osc}}$  is the oscillation period [19]. The first condition is fulfilled in our experiment, whereas the second is not. We attribute the agreement between the numerical solution and the predictions in the Raman-Nath approximation to nonlinearities, which wash out oscillations of atoms in the lattice.

Within the Raman-Nath approximation, a quite intuitive connection between the lattice

structure and its far-field diffraction pattern is possible. A BEC with initially homogeneous phase here accumulates a spatially varying phase shift  $\Delta\varphi(z) = -V(z) \cdot T/\hbar$ , and one finds that the far-field momentum distribution is  $W(p) \propto |\text{FT}(e^{i\Delta\varphi(z)})|^2$ , where FT denotes the Fourier transform with respect to  $z$  [20]. For small pulse envelopes, in which the exponential factor can be linearized, the time of flight image is directly related to the Fourier transform of the potential  $V(z)$ , i.e. the reciprocal lattice. Within second order we find  $W(p) \propto |\text{FT}(1 - iV(z) \cdot T/\hbar - (V(z) \cdot T/\hbar)^2/2)|^2$ , which allows us to express the probability to find an atom in  $\pm 1$ . diffraction orders as  $W(\pm 2\hbar k) \propto \left(\frac{S_1}{4}\right)^2 \left[1 + \left(\frac{S_2}{4}\right)^2 \pm \frac{S_2}{2} \sin \Phi\right]$  with  $S_x = V_x \cdot T/\hbar$ . The predicted sinusoidal dependence of the diffraction efficiency on the phase fits well to the experimental data shown in Fig. 4.

## II. ACKNOWLEDGMENTS

We thank P. Hänggi, D. Kölle, S. Flach, and L. Santos for discussions. We acknowledge support by the Deutsche Forschungsgemeinschaft, the Landesstiftung Baden-Württemberg and the European Community.

## III. COMPETING FINANCIAL INTERESTS

The authors declare that they have no competing financial interests.

## IV. REFERENCES

---

- [1] Dahan, M. B., Peik, E., Reichel, J., Castin, Y. & Salomon, C. Bloch Oscillations of Atoms in an Optical Potential. *Phys. Rev. Lett.* **76**, 4508 (1996).
- [2] Greiner, M., Mandel, O., Esslinger, T., Hänsch, T. W. & Bloch, I. Quantum phase transition from a superfluid to a Mott insulator in a gas of ultracold atoms. *Nature* **415**, **39** (2002).
- [3] Buonsante, P. & Vezzani, A. Phase diagram for ultracold bosons in optical lattices and superlattices. *Phys. Rev. A* **70**, 033608 (2004).

- [4] Santos, L. *et al.* Atomic Quantum Gases in Kagomé Lattices. *Phys. Rev. Lett.* **93**, 030601 (2004).
- [5] See e. g.: Hahn, Th. *International Tables for Crystallography, Volume A: Space Group Symmetry* (Reidel Publishing Company, Dordrecht, Boston, 1996).
- [6] Stützle, R. *et al.* Observation of Nonspreadng Wave Packets in an Imaginary Potential. *Phys. Rev. Lett.* **95**, 110405 (2005).
- [7] Pfau, T., Kurtsiefer, C., Adams, C. S., Sigel, M. & Mlynek, J. Magneto-optical beam splitter for atoms. *Phys. Rev. Lett.* **71**, 3427 (1993).
- [8] Mennerat-Robilliard, C. *et al.* Ratchet for Cold Rubidium Atoms: The Asymmetric Optical Lattice. *Phys. Rev. Lett.* **82**, 851 (1999).
- [9] Jacobson, J., Björk, G., Chuang, I. & Yamamoto, Y. Photonic de Broglie Waves. *Phys. Rev. Lett.* **74**, 4835 (1995).
- [10] Berman, P. R., Dubetsky, B. & Cohen, J. L. High-resolution amplitude and phase gratings in atom optics. *Phys. Rev. A* **58**, 4801 (1998).
- [11] Dubetsky, B. & Berman, P. R.  $\lambda/4$ ,  $\lambda/8$ , and Higher Order Atom Gratings Via Raman Transitions. *Laser Physics* **12**, 1161 (2002).
- [12] Weitz, M., Cennini, G., Ritt, G. & Geckeler, C. Optical multiphoton lattices. *Phys. Rev. A* **70**, 043414 (2004).
- [13] See e. g.: Meschede, D. & Metcalf, H. Atomic nanofabrication: atomic deposition and lithography by laser and magnetic forces. *J. Phys. D: Appl. Phys.* **36**, R17 (2003).
- [14] Jaksch, D., Briegel, H.-J., Cirac, J. I., Gardiner, C. W. & Zoller, P. Entanglement of Atoms via Cold Controlled Collisions. *Phys. Rev. Lett.* **82**, 1975 (1999).
- [15] Reimann, P., Grifoni, M. & Hänggi, P. Quantum Ratchets. *Phys. Rev. Lett.* **79**, 10 (1997).
- [16] Cennini, G., Ritt, G., Geckeler, C. & Weitz, M. All-Optical Realization of an Atom Laser. *Phys. Rev. Lett.* **91**, 240408 (2003).
- [17] Takasu, Y. *et al.* Spin-Singlet Bose-Einstein Condensation of Two-Electron Atoms. *Phys. Rev. Lett.* **91**, 040404 (2003).
- [18] See e. g.: Bergmann & Schäfer *Lehrbuch der Experimentalphysik: Festkörper* (de Gruyter, Berlin, 1992).
- [19] Gupta, S., Leanhardt, A. E., Cronin, A. D. & Pritchard, D. E. Coherent Manipulation of Atoms with Standing Light Waves. *C. R. Acad. Sci. Paris, t. 2, Série IV* 479 (2001).

[20] Ovchinnikov, Y. B. *et al.* Diffraction of a Released Bose-Einstein Condensate by a Pulsed Standing Light Wave *Phys. Rev. Lett.* **83**, 284 (1999).

## V. FIGURES

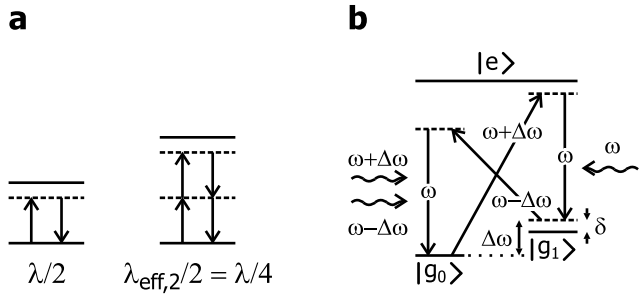


FIG. 1: Generation of lattice potentials with higher spatial periodicities. **a** Left: Virtual two-photon process in a conventional optical lattice, yielding a  $\lambda/2$  spatial periodicity of the lattice potential. Right: Virtual four-photon process contributing to a lattice potential with  $\lambda/4$  spatial periodicity. In these simple scheme however the usual lattice potential of  $\lambda/2$  periodicity due to second order processes dominates. **b** Improved scheme for generation of a four-photon lattice with  $\lambda/4$  spatial periodicity, as used in our experimental work. Compared to the four-photon process of **a**, no second order standing wave processes occur. The scheme can be generalized to lattice potentials with  $\lambda/2n$  periodicity, where  $n$  is an integer number.

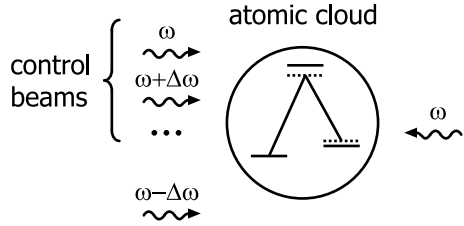


FIG. 2: Fourier synthesis of periodic atom potentials. A conventional lattice with  $\lambda/2$  spatial periodicity corresponding to the fundamental spatial frequency is realized by activating the control beam with frequency  $\omega$ , so that a standing wave at this frequency is formed. A four-photon lattice potential with  $\lambda/4$  spatial periodicity is generated when activating the control beam with frequency  $\omega + \Delta\omega$ . Along with the copropagating beam of frequency  $\omega - \Delta\omega$  and the counterpropagating beam of frequency  $\omega$ , the scheme of Fig. 1b is realized. As described in [12], further control beams of frequency  $\omega + \Delta\omega/(N - 1)$  can be added to realize higher harmonics with spatial periodicities  $\lambda/2N$  with  $N > 2$ . The phases and amplitudes of the control beams are chosen to yield the required contribution of the corresponding harmonic to the desired overall potential.

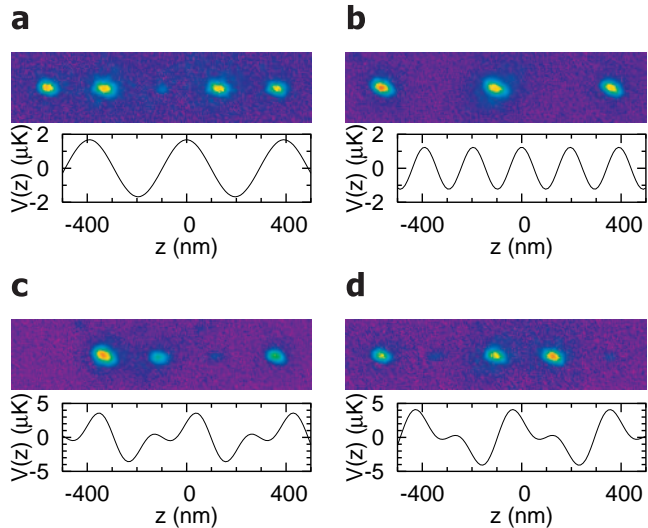


FIG. 3: Far-field diffraction images of lattice potentials and corresponding reconstructed spatial structure of the lattice potentials. **a** Two-photon lattice with  $\lambda/2$  spatial periodicity. **b** Four-photon lattice with  $\lambda/4$  spatial periodicity. Due to its smaller spatial periodicity, the splitting of the clouds is a factor two above that observed in **a**. **c** Asymmetric lattice realized by superimposing two- and four-photon lattice potentials. **d** Same as in **c**, but with an additional phase shift of  $180^\circ$  for the four-photon lattice potential.

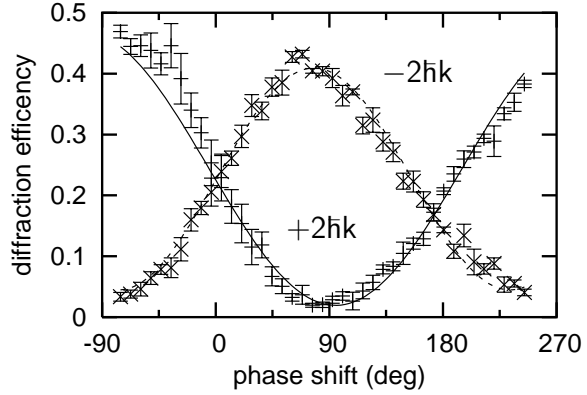


FIG. 4: Diffraction efficiency into the orders with momentum  $+2\hbar k$  (bars) and  $-2\hbar k$  (crosses) as a function of the phase shift of the four-photon component of the lattice potential. Each point corresponds to the average of 4 measurements. The data has been fitted with sinusoidal functions.